



# Effect of voltage gradient on energy consumption and chromium ions removal from salt-affected clayey soils

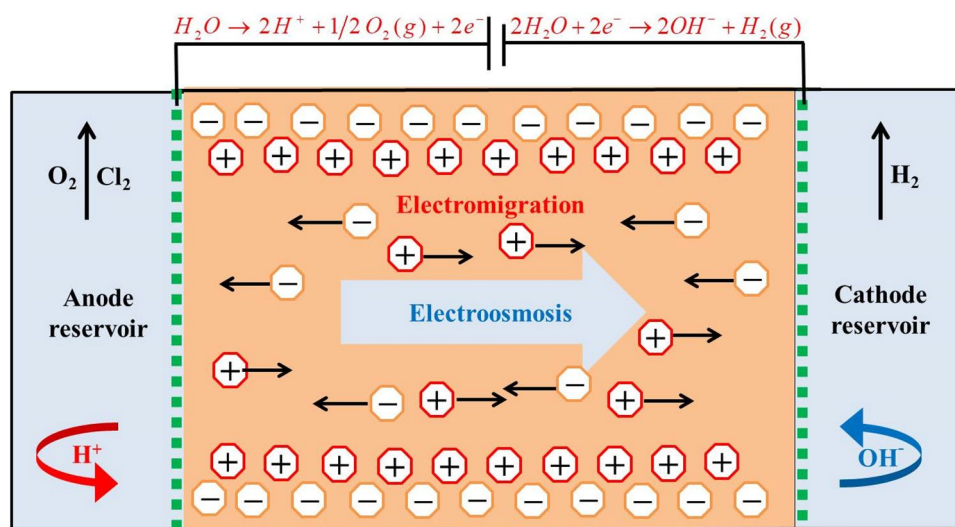
Abdul Ahad Hussain<sup>1,2</sup> · Kashif Kamran<sup>1</sup> · Muhammad Waseem<sup>1</sup> · Shahwar Umar<sup>1</sup> · Maryam Hina<sup>3</sup> · Muhammad Altaf<sup>4</sup> · **Sura Mohammad Mohealdeen**<sup>5</sup> · Mohamed A. Habila<sup>6</sup> · Ali Adhab Hussein<sup>7</sup> · Aisha Rafique<sup>1</sup>

Received: 19 May 2023 / Accepted: 2 September 2023  
© The Author(s), under exclusive licence to Springer Nature B.V. 2023

## Abstract

This study comprehensively investigates the effect of DC voltage gradient (VG) on energy consumption and the removal of ions (total Cr, Na<sup>+</sup>, Cl<sup>-</sup>, and K<sup>+</sup>) from salt-affected clayey soil. In this work, different VG (i.e., 0.5, 1, and 2 V cm<sup>-1</sup>) were applied over the artificially contaminated soil for 48 h during electrokinetic experiments to determine the electric potential distribution, electroosmotic flow (EOF), and electric current variation. The results revealed that the VG directly influences the EOF rate and electromigration of ionic species present in the pore solution of the soil samples. The higher removal of ions was achieved with the intensity of applied electric field (EF) due to electromigration and higher EOF rate. Therefore, the maximum ion removal was achieved at 2 V cm<sup>-1</sup> [i.e., total Cr (71%), Na<sup>+</sup> (91%), Cl<sup>-</sup> (64%), and K<sup>+</sup> (63%)]. In addition, the EOF rate decreased with increasing treatment time, which was attributed to the progression of acidic-alkaline fronts in soil samples. The collision of acidic-alkaline fronts resulted in a large VG in a narrow soil region of pH jump reducing the EOF and electromigration of ions. Regardless of low EF (i.e., 0.5 V cm<sup>-1</sup>), the EOF rate and removal of ions decreased [i.e., total Cr (36%), Na<sup>+</sup> (58%), Cl<sup>-</sup> (45%), and K<sup>+</sup> (37%)]. Moreover, the higher EF (i.e., 2 V cm<sup>-1</sup>) resulted in higher energy consumption (218.6 kWh m<sup>-3</sup>) and a reduction in the electrical conductivity of soil from 5.2 to 1.29 dS m<sup>-1</sup>.

## Graphical abstract



**Keywords** Electric potential · Acidic-alkaline fronts · Heavy metal · Electrical conductivity · Energy consumption

Extended author information available on the last page of the article

## 1 Introduction

Chromium (Cr) exists in several types of oxidation states, but the most common and steady states are hexavalent Cr(VI) and trivalent Cr(III) [1]. Usually, the Cr(VI) occurs in the form of chromate and dichromate ions (i.e.,  $\text{CrO}_4^{2-}$ ,  $\text{Cr}_2\text{O}_7^{2-}$  and  $\text{FeO}(\text{Cr}_2\text{O}_3)$ ), while the Cr(III) occurs in cations (i.e.,  $\text{Cr}_3(\text{OH})_4^{5+}$  and  $\text{CrOH}^{2+}$ ), which are vastly carcinogenic to living organisms [2, 3]. Cr(VI) is widely used in industrial applications such as steel manufacturing, leather processing, fabric dyeing, and electroplating, resulting in the release of chromium-contaminated wastes into soil, water, and air due to poor waste leaching and unintentional spills [4]. Cr(VI) is highly soluble in water and can be included in the food chain via vegetables, fruits and fresh water. Usually, the Cr concentration in sea and fresh water varies from 0.5 to 50  $\mu\text{g L}^{-1}$  and 0.1 to 117  $\mu\text{g L}^{-1}$ , respectively [5]. In addition, naturally, the Cr concentration in the soil varies from 10 to 50  $\text{mg kg}^{-1}$  but in agricultural soils, this concentration may reach up to 350  $\text{mg kg}^{-1}$  [6]. Cr(VI) is the most harmful in all oxidation states, causing DNA, membrane lipids, cellular integrity, and effects on the kidney, liver, respiratory system, and skin cancer [7, 8]. Due to these circumstances, the desalination of agricultural soil is essential.

Several researchers have proposed various methods for removing heavy metals and organic contaminants from contaminated soil and water in situ and ex situ, such as electrokinetics (EK) [9]. It is one of the most precious methods for the reclamation of low-permeable contaminated soils. In 1930, the first EK experiment was conducted in India by Puri and Anand for the reclamation of sodium-affected alkaline soil [10].

The EK remediation technique involves inserting the electrodes over the contaminated soil and applying a DC electric field (EF) via the electrodes [11, 12]. The main transport mechanisms in EK are electromigration (migration of ions), electrophoresis (movement of charged particles), and electroosmosis (movement of water) [13, 14].

The EK method has some benefits and drawbacks over former technologies, such as easy to handle, fast, and usable in both lab and field-scale experiments. However, on the other side, electrode corrosion, high buffering capacity, focusing, and thermal effects, as well as precipitation of ions are the main limiting factors in the EK method [15].

To optimize the removal of contaminants, living organisms should be kept alive. Under the application of a potential gradient, the pH and thermal effect (Joule heating effect) are the main parameters for attaining a suitable environment for the organisms [16, 17].

During the EK process, proton ( $\text{H}^+$  ions) and hydroxyl ( $\text{OH}^-$  ions) ions are generated by the electrolysis of water

on the anode and cathode sides, respectively [18, 19]. To attain the neutral state, these ions move toward the opposite electrodes via soil media due to electroosmosis and electromigration processes [13]. However, the acidic and alkaline fronts have different consequences in soil, such as the adsorption of  $\text{H}^+$  ions on soil particles at anode side which causes a reduction in electroosmotic flow (EOF). In addition, the  $\text{OH}^-$  ions cause the precipitation of metal ions in the form of hydroxyl and carbonate complexes by reducing the pore space in soil [17, 20]. Therefore, in order to create a favorable habitat for microorganisms, it is imperative that the soil pH falls within the range of 3 to 9 [21].

However, in circumstances of extreme acidity and alkalinity, the growth of microorganisms is inhibited by distortion in microbial metabolism, low nutrient availability in soil and pore water [17, 21]. Therefore, many researchers have suggested different methods such as buffer solutions and chelating agents can be used on anode and cathode sides to maintain the pH value for biological and EK remediation of soil [22].

Particularly, the main challenge is to find a life-compatible and environment-friendly reagent effective in both the anode and the cathode pH regulation. This strategy is not easy to apply due to cost-effective and fail to long-term treatments. A different strategy is the low EF intensity applied to the contaminated soil. Initially, this is a simple solution for reducing the changes in the pH of soil [23–24].

In former studies, EK effects with different VG have been studied either to remove the salts (i.e., Na,  $\text{Ca}^+$ , and K) from saline-sodic soil [25], organic materials (i.e., diesel hydrocarbons) from clay soil [26] or only heavy metals (i.e., Pb and Cd) from loess [27], fluorine from red mud [28], and Cr(VI) from zeolite [29].

The aim of this study was to investigate the feasibility of different VG (0.5, 1, and 2  $\text{V cm}^{-1}$ ) on energy consumption and the removal of heavy metal (i.e., total Cr) and salt ( $\text{Na}^+$ ,  $\text{Cl}^-$ , and  $\text{K}^+$ ) ions from salt-affected clayey soils. For this purpose, the soil samples were artificially contaminated with 3.7  $\text{g kg}^{-1}$  of NaCl and 1.9  $\text{g kg}^{-1}$  of  $\text{K}_2\text{Cr}_2\text{O}_7$ . Since the changes in soil's pH, current, and electric potential distribution play a significant role in determining the effective EK energy consumption and removal of ions, therefore, these factors were measured during experiments by applying a continuous EF over the soil specimens via iron mesh electrodes.

## 2 Materials and methods

### 2.1 Soil sample

In this study, the soil was collected at depth of ~0–20 cm from an agriculture field near Sheikhpura, Punjab, Pakistan

(31° 42' 40" N, 73° 59' 16" E). The soil was air dried at room temperature. Three soil samples were taken to determine the physicochemical properties of soil and the average values are given in Table 1.

The hydraulic permeability of soil was determined by the Darcy's law using the constant-head method, while the hydraulic flux ( $V$ ) of soil was determined by the following Eq. [ $V = Ki$ ] [30] where "K" is the hydraulic permeability ( $\text{cm s}^{-1}$ ) and "i" is the hydraulic gradient (–).

The bulk density ( $B$ ) of soil was determined by the core method using the following Eq. [ $B = \frac{M_b}{V_b}$ ], where " $M_b$ " is the mass of oven-dry soil (g) and " $V_b$ " is the volume of soil ( $\text{cm}^3$ ) [31].

Whereas, the particle density ( $P$ ) was determined by the graduated cylindrical method using the following Eq. [ $P = \frac{M_p}{V_p}$ ]: where " $M_p$ " is the mass of oven-dry soil (g) and " $V_p$ " is the volume of solids ( $\text{cm}^3$ ) [31]. The mean value of soil porosity was determined by Eq. (1) [30].

$$\text{Soil porosity(\%)} = \left( 1 - \frac{\sum_{i=1}^n B_i}{\sum_{i=1}^n P_i} \right) \times 100 \quad (1)$$

where, " $\sum_{i=1}^n B_i$ " is the sum of all values of bulk density and " $\sum_{i=1}^n P_i$ " is the sum of all values of particle density.

**Table 1** The physiochemical properties of collected soil

Measurements	Results
Hydraulic permeability	$1.71 \times 10^{-6} \text{ cm s}^{-1}$
Hydraulic flux	$7.1 \times 10^{-6} \text{ cm s}^{-1}$
Bulk density	$1.12 \text{ g cm}^{-3}$
Particle density	$1.42 \text{ g cm}^{-3}$
Soil porosity	21%
Standard deviation of porosity	3.35
Moisture content	2%
EC <sub>1:2</sub>	$1.22 \text{ dS m}^{-1}$
pH <sub>1:2</sub>	8.1
Organic matter	3.52%
Soil type	Clay
Grain size distribution	
Clay	59%
Sand	25.5%
Silt	15.5%
Initial ionic concentration	
Total Cr	Nil
Fe <sup>+2</sup>	$0.351 \text{ g kg}^{-1}$
Na <sup>+</sup>	$0.561 \text{ g kg}^{-1}$
K <sup>+</sup>	$0.23 \text{ g kg}^{-1}$
Cl <sup>-</sup>	$0.697 \text{ g kg}^{-1}$
Ca <sup>+2</sup>	$0.376 \text{ g kg}^{-1}$

To determine the moisture content in soil, 20 g of soil was taken and dried at  $105 \pm 5$  °C for 24 h and the mass of the dried soil was noted. The moisture content was calculated by Eq. (2) [31].

$$\text{Soil moisture(\%)} = \left( \frac{M_w}{M_d} - 1 \right) \times 100 \quad (2)$$

where " $M_w$ " is the mass of wet soil (g) and " $M_d$ " is the mass of dry soil (g).

Thereafter, to determine the soil's electrical conductivity (EC) and pH, the soil and distilled water ratio was used (1:2). The EC and pH was measured by the EC meter (HANNA, HI99300) and pH meter (HANNA, HI2002-01), respectively. To determine the concentration of Cl<sup>-</sup> ions, we prepared a suspension of soil and distilled water in a graduated flask with a ratio of (1:5). The suspension was placed on a rotary shaker (Model-1050) for 1 h and then filtered by filter paper (Whatman, grade 42). The concentration of Cl<sup>-</sup> ions was calculated by argentometric titration [30, 32]. To extract the Na<sup>+</sup>, K<sup>+</sup>, and Ca<sup>+2</sup> ions from soil, 10 g of soil was stirred with 50 ml of 1 N ammonium acetate solution (NH<sub>4</sub>OAc) at 150 rpm for 1 h and filtered with filter paper (Whatman, grade 1). The concentrations of Na<sup>+</sup>, K<sup>+</sup>, and Ca<sup>+2</sup> were determined by a flame-photometer (Sherwood, 360). To prepare the 1 N NH<sub>4</sub>OAc solution, we added 57 and 68 ml of concentrated acetic acid and ammonium hydroxide, respectively, into the 800 ml of distilled water and maintained the pH of the solution at 7 by adding more acetic acid and ammonium hydroxide [31].

The total Cr and Fe<sup>+2</sup> ions were extracted via the block-digester digestion method using concentrated HF, HCl, and HClO<sub>4</sub>. Therefore, 1 g of soil was mixed with 5 ml of distilled water and 2 ml of HClO<sub>4</sub> and HF, and heated to near dryness. Thereafter, more 2 and 8 ml of HClO<sub>4</sub> and HF were added, respectively, and heated to near dryness. Then 8 ml of HCl and 20 ml of distilled water were added to the residue. A further 75 ml of distilled water was added to bring the volume of the extracted solution to 100 ml and which was stored in a plastic bottle [31]. The concentration of total Cr and Fe<sup>+2</sup> was determined by atomic absorption spectroscopy (AAS) [33].

The organic content and soil particle size distribution were determined by the loss on ignition method [34] and the hydrometer method [35], respectively. The results depict that the soil type is clay, based on the grain size distribution.

## 2.2 Electrokinetic setup and sample preparation

The diagram of the EK setup is shown in Fig. 1. The EK cell comprises three sections, in which the soil section is sandwiched between the electrode sections (i.e., anode and cathode). The filter paper was inserted between the electrodes

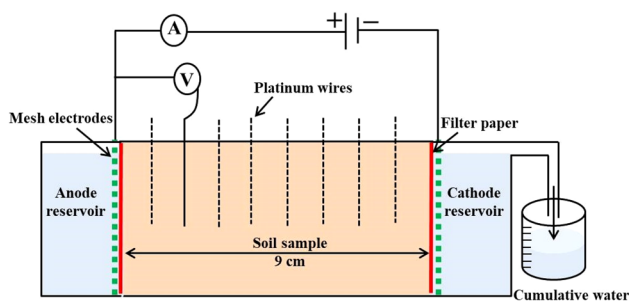


**Fig. 1** Schematic diagram of the electrokinetic setup for reclamation of chromium-contaminated salt-affected soils

and soil sample to avoid the movement of wet soil particles into the electrode section. The EK cell was made from an acrylic plexiglass sheet with a 7 mm thickness. The volume of the soil section was  $9 \text{ (L)} \times 6.9 \text{ (W)} \times 7.3 \text{ (H)} \text{ cm}^3$ , while the volume of the electrode section was  $9.8 \text{ (L)} \times 9.2 \text{ (W)} \times 7.5 \text{ (H)} \text{ cm}^3$ .

In this study, we performed the three EK experiments (E-1, E-2, and E-3) with different VG ( $0.5, 1, \text{ and } 2 \text{ V cm}^{-1}$ ), respectively, for 48 h. For each EK experiment, 670 g of dry soil was used. To prepare the contaminated soil,  $3.7 \text{ g kg}^{-1}$  of NaCl (CAS No. 7647-14-5, DAEJUNG) and  $1.9 \text{ g kg}^{-1}$  of  $\text{K}_2\text{Cr}_2\text{O}_7$  (CAS No. 7778-50-9, DAEJUNG) were used. The saturated paste of soil was prepared, mixed with a known amount of salts and 227 ml of distilled water, and placed in the soil section of the EK cell. Each electrode section was filled with 710 ml of distilled water. In this study, iron mesh electrodes were used to provide an EF over the soil specimens. To avoid the effect of corrosion, mesh electrodes were changed frequently after 16 h up to the completion of experiments (i.e., 48 h).

To measure the electric potential distribution, platinum wires were introduced into the soil sample every centimeter and connected in parallel with the LabJack (U12), while the variation in current was measured by the digital-multimeter. The pH of the electrode sections was measured by the pH meter and pH strips were used to track the pH changes in the soil. During the EK experiment, the water was collected in the graduated beaker at the cathode side due to electroosmosis.

### 2.3 Soil analysis

After the completion of EK experiments, the soil samples were immediately segmented into nine equal parts and dried in a dry oven (DHG-9030 A) at  $105 \pm 5 \text{ }^\circ\text{C}$  for 7 h. To determine the EC and  $\text{Cl}^-$  ions, the soil and distilled water ratio was kept (1:2). The EC and concentration of  $\text{Cl}^-$  ions were measured by the EC meter and argentometric titration, respectively [32].

To extract the  $\text{Na}^+$  and  $\text{K}^+$  ions, the soil and 1 N of  $\text{NH}_4\text{OAc}$  solution ratio was kept (1:5). The extractable  $\text{Na}^+$  and  $\text{K}^+$  were determined by a flame-photometer. In addition, the total Cr and  $\text{Fe}^{+2}$  were extracted via the block-digester digestion method [3] and concentration of total Cr and  $\text{Fe}^{+2}$  ions was determined by AAS [33].

## 3 Results and discussion

### 3.1 Electric potential, current, pH of soil and water reservoirs

In this part of research, the electric potential distribution, current, and pH variation in soil and water reservoirs during three EK experiments (i.e., E-1, E-2, and E-3) were noted. The three EK experiments were conducted for 48 h with different VG, i.e.,  $0.5, 1, \text{ and } 2 \text{ V cm}^{-1}$ . The electric potential distribution in soil samples for 48 h is shown in Fig. 2a–c. The initial profiles (at  $t=0 \text{ h}$ ) of electric potential in all experiments indicate the linearity instead the region of both electrodes (i.e., anode and cathode). The linear profiles show the homogeneous concentration of water, salts, and metal ions in the contaminated soil. While, the potential drop over the electrodes shows the soil-electrode interfaces, which indicates the less number of charges in the electrode compartments to carry the current because electrodes dipped into the distilled water [36]. Therefore, the initial values (at  $t=0 \text{ h}$ ) of electric current were low during all experiments as shown in Fig. 2d. The initial values of the current were 62 mA, 151 mA, and 321 mA, during E-1, E-2, and E-3, respectively. However, quickly the potential drop over the soil-electrode interfaces decreases and the maximum current passes through the soil samples due to the migration of ionic species toward the electrodes by electromigration and EOF [3].

The potential profile during E-1 (i.e., Fig. 2a) shows that the linearity sustains up to the end of EK experiment (48 h) and current progressively decreases due to the absence of high pH jump within the soil sample. While, during E-2 and E-3, the potential profiles (i.e., Fig. 2b, c) deviate from its linear position after 10 and 4 h, respectively, and current also decreases due to the high formation of  $\text{H}^+$  (acid front) and  $\text{OH}^-$  (basic front) ions within the soil samples. Thereafter, a sharp potential drop (i.e., focusing effect or electro-neutrality region) was observed by the collision of  $\text{H}^+$  and  $\text{OH}^-$  ions in the soil samples at the  $\sim 1/3$  part from the anode side after 10 and 20 h, respectively, as shown in Fig. 2b, c. This phenomena is also observed in the desalination of fired-clay bricks by Ishaq et al. [32] and Kamran et al. [37], where removal of ions were stagnated.

During E-3, the development of a sharp potential drop 10 h early as compared to the E-2 due to the high formation

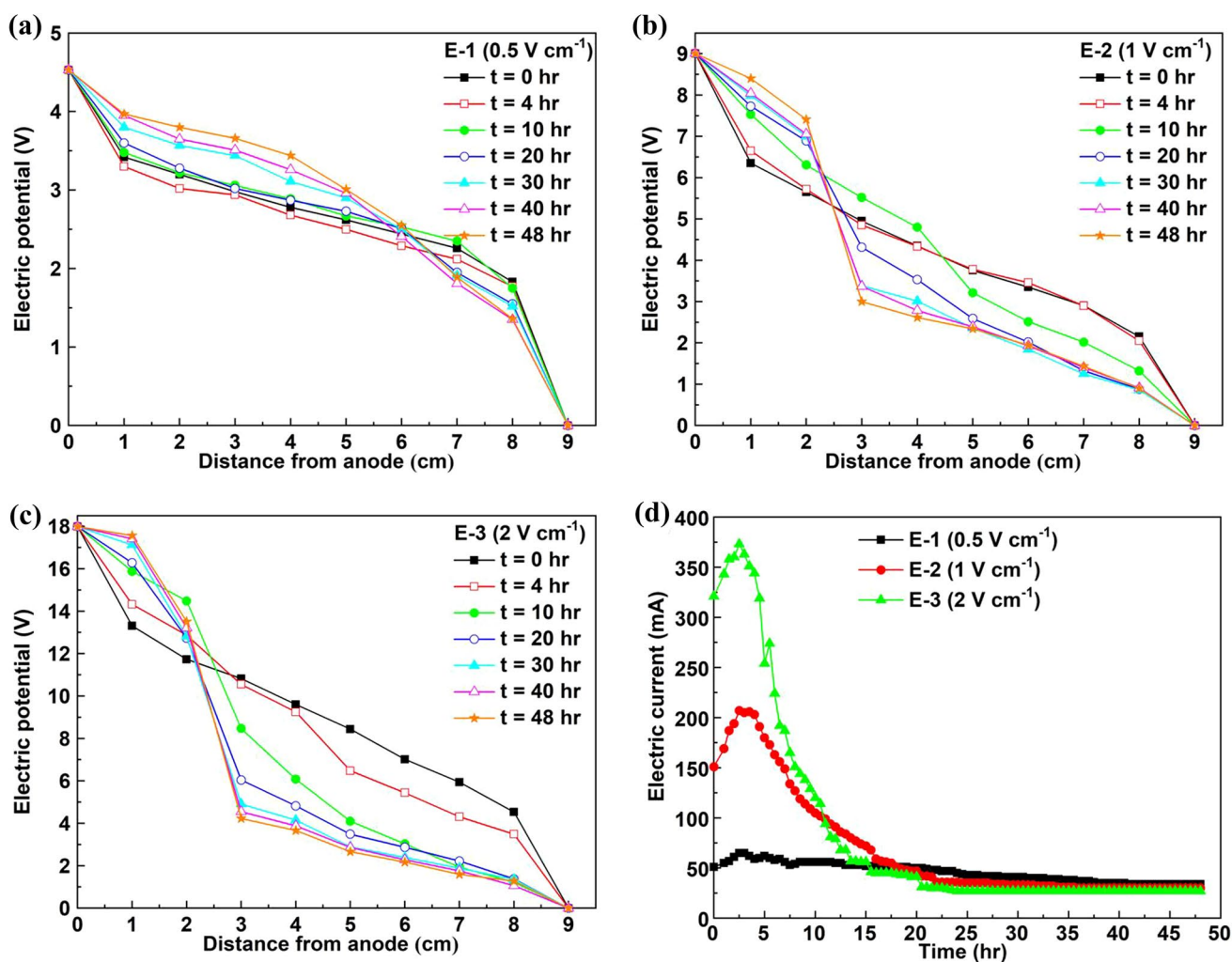


**Fig. 2** The electric potential **a** E-1, **b** E-2, **c** E-3, and electric current **d** in soil samples for E-1, E-2, and E-3 experiments after applying the electric fields of 0.5, 1, and 2 V cm<sup>-1</sup> over the soil samples

of H<sup>+</sup> and OH<sup>-</sup> ions by the higher EF. A similar trend of potential was noted by Hussain et al. within the soil and observed that the EOF rate and migration of Pb<sup>2+</sup> ions were stopped by the collision of H<sup>+</sup> and OH<sup>-</sup> ions [30]. Similarly, in our case the EOF and migration of ions may be stopped by the collision of acidic-alkaline fronts in the soil under high EF.

After applying the EF, the H<sup>+</sup> and OH<sup>-</sup> ions produce at anode and cathode reservoir, respectively, by electrolysis, therefore the pH of the anode and cathode water reservoirs is shown in Fig. 3a. The initial pH of the anode and cathode water reservoirs was almost 7 because distilled water was used for each EK experiment. The red lines depict the variation in acidic environment (i.e., H<sup>+</sup> ions) at the anode reservoir, while the blue lines depict the variation in alkaline environment (i.e., OH<sup>-</sup> ions) at the cathode reservoir.

To the EF of 0.5 V cm<sup>-1</sup> (i.e., E-1), the pH of the anode and cathode reservoirs changed from ~7 to ~4 and ~7 to

~9.1 within 4 and 12 h, respectively, while during E-2 (i.e., 1 V cm<sup>-1</sup>), the pH of the anode and cathode reservoir varied from ~7 to ~3 and ~7 to ~13 within 22 and 25 h, respectively. During the EF of 2 V cm<sup>-1</sup> (i.e., E-3), the pH of the anode reservoir decreased from ~7 to ~2.9 and to the cathode reservoir the pH varied from ~7 to ~13 within 7 and 14 h, respectively, and these values did not change up to the end of experiment. This difference in the pH values show that the initial applied EF over the soil samples influences the production rates of the H<sup>+</sup> and OH<sup>-</sup> ions at the anode and cathode reservoirs, respectively.

The H<sup>+</sup> and OH<sup>-</sup> ions concentration depends on the presence of ionic concentration in soil and the intensity of the applied EF, so the formation of the acidic-alkaline environment increased with treatment time at the anode and cathode. Based on the Faraday's law of mass and charge equation, the rate at which ions are formed at electrode is expressed in Eq. (3) [38].

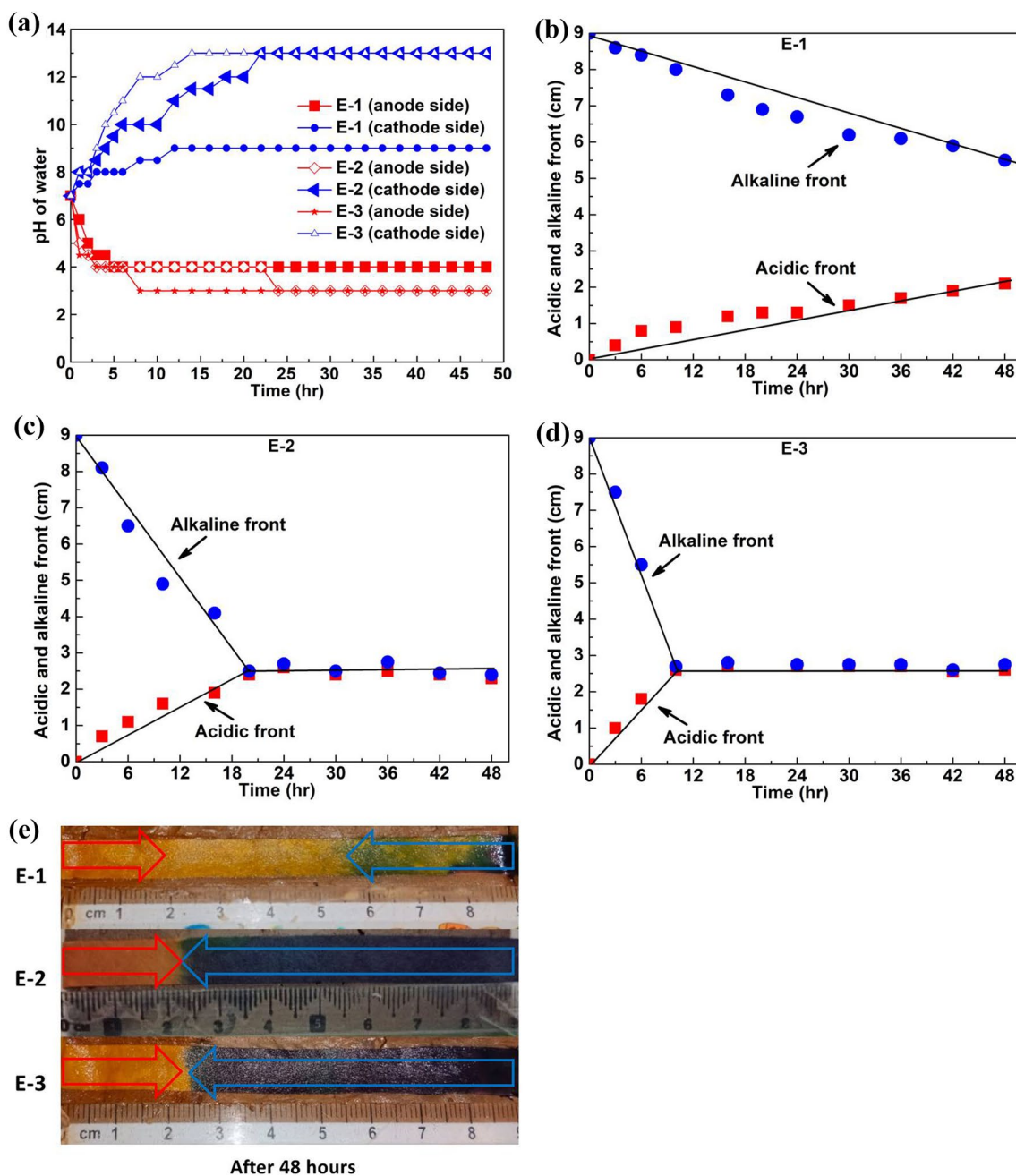


**Fig. 3** pH variation in the anode and cathode reservoirs **a** acidic-alkaline front positions in soil **b** E-1, **c** E-2, and **d** E-3 during electrokinetic experiments for 48 h. The pH changes in the soil samples after

the all electrokinetic experiments (i.e., 48 h) is shown in **e**. Red color of the pH strips depicts the acidic environment while blue color of the pH strips depicts the alkaline environment. (Color figure online)

$$\text{Molar flux}(\text{mols}^{-1}\text{cm}^{-2}) = \frac{J}{Z \times F} \quad (3)$$

where, “ $J$ ” is the current density ( $\text{A cm}^{-2}$ ), “ $Z$ ” is the ionic valence (–), and “ $F$ ” is the Faraday’s constant ( $96,485 \text{ C mol}^{-1}$  electrons).

However, with the passage of time, the  $\text{H}^+$  and  $\text{OH}^-$  ions moved toward the cathode and anode sides, respectively, via

soil samples. Therefore, the pH changes (i.e.,  $\text{H}^+$  (acid) and  $\text{OH}^-$  (alkaline) front’s positions) in the soil was tracked by pH strips during different treatment time up to 48 h as shown in Fig. 3b–d. The red profiles in Fig. 3b–d depict the  $\text{H}^+$  ion positions while the blue profiles depict the  $\text{OH}^-$  ion positions in the soil samples. Under the lower EF of  $0.5 \text{ V cm}^{-1}$  (i.e., E-1), the  $\text{H}^+$  and  $\text{OH}^-$  fronts reached up to  $\sim 2$  and  $\sim 5.5$  cm in the soil sample from anode side, respectively, within 48 h.

It can be seen in Fig. 3b, the collision of  $H^+$  and  $OH^-$  fronts did not occur due to the low production rate of  $H^+$  and  $OH^-$  ions as well as their slow movement due to low EF ( $0.5 \text{ V cm}^{-1}$ ). Whereas in E-2 and E-3, the  $H^+$  and  $OH^-$  fronts collided with each other at  $\sim 2.3 \text{ cm}$  from anode side after 20 and 10 h, respectively, and stagnated their migration up to the end of experiments (48 h). The pH changes in soil after 48 h of experiment are shown in Fig. 3e. The red color of the pH strips depicts the acidic nature of soil while blue color of the pH strips depicts the alkaline nature of soil. The progression of the acidic environment was limited near the anode, although the mobility of  $H^+$  ions is 1.8 times faster than that of  $OH^-$  ions, while the direction of EOF directed from anode to cathode [13]. This behavior is related to several factors, such as the initial high soil pH (i.e., 8.1), the high buffering capacity of soil against acidic environment and the formation of hydroxide compounds (i.e., NaOH and KOH) [39].

### 3.2 Electroosmosis

During EK experiments, the EOF was collected from cathode side, which shows that soil particle has a net negative charge. The effect of different VG (i.e., 0.5, 1, and  $2 \text{ V cm}^{-1}$ ) on the EOF rate and cumulative EOF is shown in Fig. 4a, b. The EOF rate for each EK experiment was calculated by the following Eq. (4) [40].

$$\text{Electroosmotic flow rate (ml h}^{-1}\text{)} = \frac{V}{t} \quad (4)$$

Where, “ $V$ ” is the total collected volume of water (ml) and “ $t$ ” is the treatment time (h).

We can see in Fig. 4a, initially, the EOF rate was high in all EK experiments due to the high water content and the absences of acidic-alkaline fronts in the soil samples. Since, with the

passage of time, the EOF rate decreased due to the progression of  $H^+$  and  $OH^-$  ions therefore, the EOF rate decreased due to the low pH value ( $< 3$ ) at the anode side. Hussain et al. also reported that the electroosmosis dewatering performed better at higher pH value ( $> 3$ ) [41]. In addition, the adsorption of cations (i.e.,  $H^+$ ,  $Na^+$ , and  $Fe^{+2}$  ions) with soil particles reduced the thickness of diffuse double layer (DDL) [42] and made the soil zeta potential less negative thus decreased the EOF rate [19]. Moreover, the maximum cumulative EOF was observed in E-2 (i.e., Fig. 4b), where  $1 \text{ V cm}^{-1}$  was applied over the soil sample. In this case, the net EOF of water was  $\sim 94 \text{ ml}$  after 48 h. It can be seen in Fig. 4b, the EOF almost stopped after 32 h by the collision of pH fronts within the soil. However, at higher EF (i.e.,  $2 \text{ V cm}^{-1}$ ), the EOF decreased (i.e.,  $\sim 69$ ) by reduction in DDL and the formation of a higher potential drop within the soil after 10 h.

The minimum cumulative EOF ( $\sim 64 \text{ ml}$ ) was observed during E-1, where lower EF, i.e.,  $0.5 \text{ V cm}^{-1}$  was applied over the soil sample. During E-1, the cumulative EOF was not decreased due to the absence of high pH jump; therefore the EOF profile has a linear up to 48 h. In E-1, the EOF may surpass E-2 and E-3 if prolong the treatment time; hence, the high removal of ions was achieved by the continuous EOF rate. The net EOF of water with respect to different applied EF is shown in the inset of Fig. 4b.

The permeability of the soil depends on the water flow rate and the applied EF strength. The electroosmotic permeability of soil with respect to different treatment times is shown in the inset of Fig. 4a and determined by Eq. (5) [30].

$$\text{Electroosmotic permeability (cm}^2 \text{ V}^{-1} \text{ s}^{-1}\text{)} = \frac{VL}{EtA} \quad (5)$$

Where, “ $V$ ” is the total collected volume of water (ml), “ $L$ ” is the length of soil sample (cm), “ $E$ ” is the electric

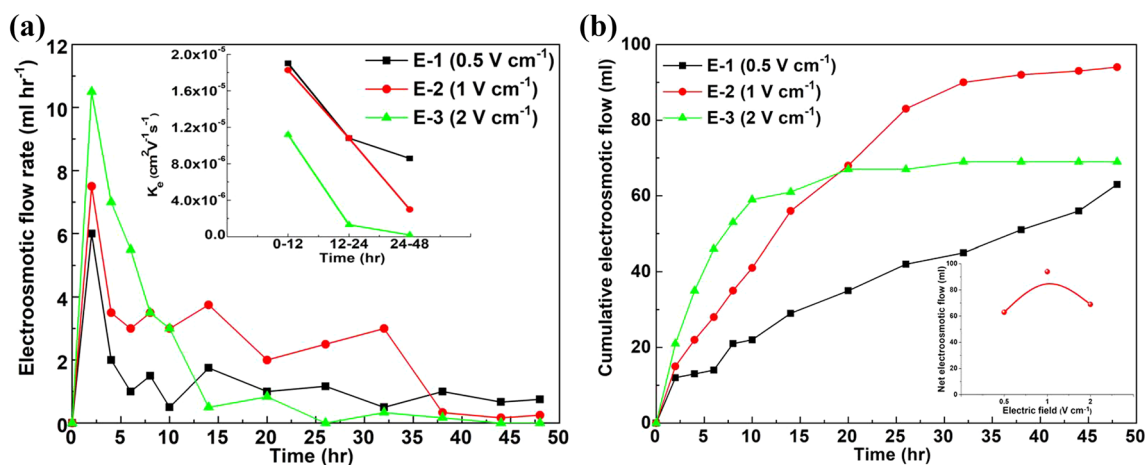


**Fig. 4** The electroosmotic flow rate **a** and cumulative electroosmotic flow **b** after applying the electric field of 0.5, 1, and  $2 \text{ V cm}^{-1}$  over the soil samples during all electrokinetic experiments. The electroos-

motomic permeability of soil is shown in the inset of Fig. 4a, while the net electroosmotic flow of water after 48 h is shown in the inset of Fig. 4b

potential (V), “ $t$ ” is the treatment time (h), and “ $A$ ” is the area of soil sample ( $\text{cm}^2$ ). The electroosmotic permeability of the soil changes with different applied EF strengths was due to the progression of acidic-alkaline environments. The electroosmotic permeability of soil after 48 h of experiments during E-1, E-2, and E-3 was  $1.175 \times 10^{-5}$ ,  $8.76 \times 10^{-6}$ , and  $3.21 \times 10^{-6} \text{ cm}^2 \text{ V}^{-1} \text{ s}^{-1}$ , respectively.

### 3.3 The variation in ions distribution and electrical conductivity in soil

The ionic concentrations of total Cr,  $\text{Fe}^{+2}$ ,  $\text{Na}^+$ ,  $\text{Cl}^-$ , and  $\text{K}^+$  in soil as well as EC of soil samples before and after the completion of E-1, E-2, and E-3 experiments with different applied VG (i.e., 0.5, 1, and  $2 \text{ V cm}^{-1}$ ) are shown in Fig. 5a–f. It can be seen in Fig. 5a–f, the dashed lines represent the initial ionic

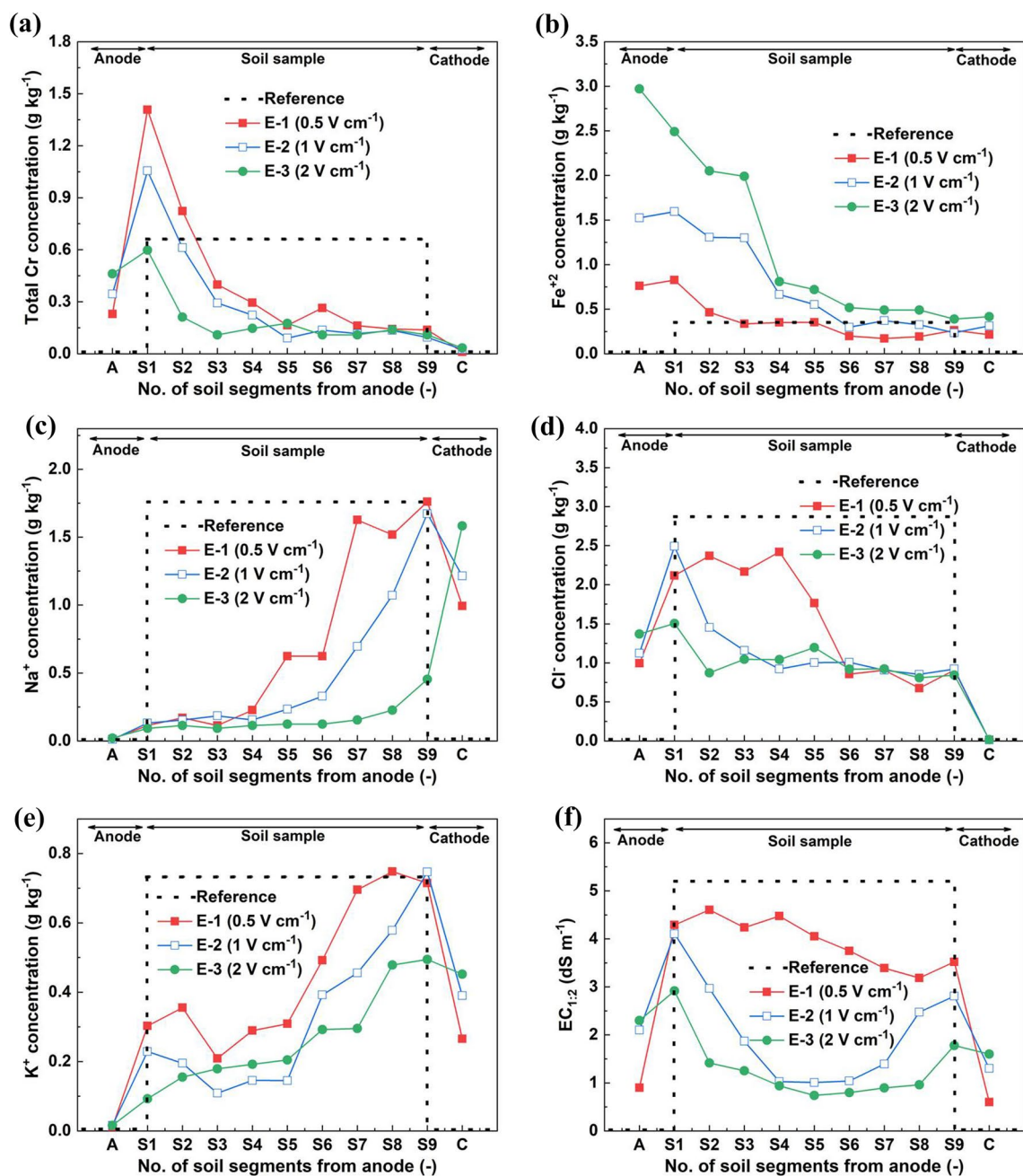


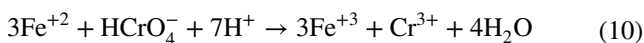
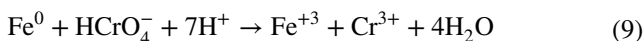
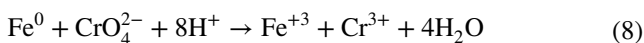
**Fig. 5** The concentrations of total Cr (a),  $\text{Fe}^{+2}$  (b),  $\text{Na}^+$  (c),  $\text{Cl}^-$  (d),  $\text{K}^+$  (e), and EC (f) in soil segments before and after the all electrokinetic experiments

concentration in soil segments and electrode reservoirs (anode and cathode) before the all EK experiments.

The total Cr profiles (i.e., Fig. 5a) indicate that the Cr(VI) migrates toward the anode due to the electromigration and diffusion process in the form of oxygen anion or chromate ions, i.e.,  $\text{CrO}_4^{2-}$ ,  $\text{HCrO}_4^-$ , and  $\text{Cr}_2\text{O}_7^{2-}$  [3]. Therefore, the Cr(VI) may convert into the deoxidized and less toxic form Cr(III) according to following Eq. (6) [43].



In this work, the iron mesh electrodes were used to apply the EF over the soil samples. Therefore,  $\text{Fe}^{+2}$  ions produced by oxidation and moved toward the cathode due to the electromigration and EOF. The variation in  $\text{Fe}^{+2}$  ion profiles before and after EK experiments is shown in Fig. 5b. After each experiment, the higher concentrations of  $\text{Fe}^{+2}$  ions were observed in soil samples as compared to reference line which indicate the  $\text{Fe}^{+2}$  ions moved toward the cathode via soil samples. During EK experiments, the chromate ions may react with the  $\text{Fe}^0$  and  $\text{Fe}^{+2}$  ions to reduce the Cr(VI) to Cr(III) (i.e., less toxic form) according to following Eqs. (7, 8, 9, 10) [2, 19, 44, 45].



In EK experiments, the  $\text{H}^+$  and  $\text{Fe}^{+2}$  ions may cause the adsorption of Cr(VI) at the vicinity of anode within soil samples [46]. Therefore, the precipitation and accumulation of Cr(VI) are higher in more acidic environment as a result of the lower removal of Cr ions.

However, the distribution of  $\text{Na}^+$  and  $\text{K}^+$  ions in soil samples after the each EK experiment is shown in Fig. 5c, e. Under the influence of the applied EF (i.e., 0.5, 1, and 2  $\text{V cm}^{-1}$ ), the  $\text{Na}^+$  and  $\text{K}^+$  ions moved toward the cathode reservoir and accumulated over there. It can be seen in Fig. 5c, e, the removal of ions is higher at the anode side with respect to the number of soil segments due to the electromigration, EOF, and diffusion process [47].

In the case of  $\text{Cl}^-$  ions, the  $\text{Cl}^-$  ions moved toward the anode due to the electromigration and diffusion. Therefore, due to the oxidation reaction at anode, some chloride ions accumulate in the anode water reservoir and some ions are converted into  $\text{Cl}_2$  gas according to following Eq. (11) [48].



The variation in removal efficiencies of total Cr,  $\text{Na}^+$ ,  $\text{Cl}^-$ , and  $\text{K}^+$  ions from soil for E-1, E-2, and E-3 after the completion of EK experiments (i.e., 48 h) is shown in Fig. 6.

The EC of soil depends on the total concentration of ionic species in the soil [30]. The EC of soil after each experiment is shown in Fig. 5f. The dashed line represents the initial value of EC (i.e.,  $\text{EC}_{1,2} = 5.2 \text{ dS m}^{-1}$ ) in soil before the EK experiments. After applying the EF, the ionic species move toward the respective electrodes due to the electromigration, EOF, and diffusion processes, so the value of EC decreases in the vicinity of the central part of the soil and increases in the vicinity of anode and cathode side. The results demonstrate that the maximum number of ionic species was removed when an EF of 2  $\text{V cm}^{-1}$  was applied over the soil sample. The residual and reduction in EC of soil after each EK experiment is given in Table 2.

### 3.4 Removal efficiency of ions and energy consumption

The removal efficiency (RE) of ions and energy consumption depend on the applied EF strength [33]. Both parameters are significant to calculate the feasibility of EK for the extraction of contaminants from polluted soil. The removal efficiencies of ions (i.e., total Cr,  $\text{Na}^+$ ,  $\text{Cl}^-$ , and  $\text{K}^+$  ions), EC of soil, and energy density after 48 h of each EK experiment are shown in Fig. 6 and their values are given in Table 2. The removal efficiencies of ions was calculated by Eq. (12) [32].

$$\text{RE} = \left( \frac{\sum_{i=1}^9 C_i - \sum_{f=1}^9 C_f}{\sum_{i=1}^9 C_i} \right) \times 100\% \quad (12)$$

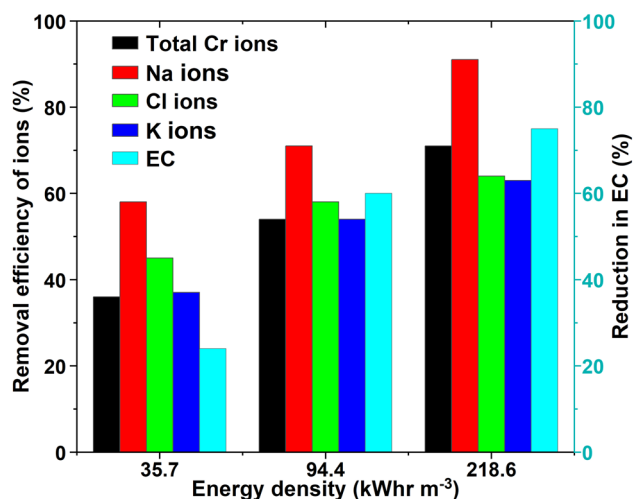


Fig. 6 Removal efficiency of ions and reduction in EC of soil after the all electrokinetic experiments

**Table 2** The removal efficiency of total Cr, Na<sup>+</sup>, Cl<sup>-</sup>, and K<sup>+</sup> ions, the reduction in EC of soil, the cumulative water flow, and energy density after the all electrokinetic experiments

Experiments (electric field V cm <sup>-1</sup> )	Total Cr removal efficiency (%)	Na <sup>+</sup> removal efficiency (%)	Cl <sup>-</sup> removal efficiency (%)	K <sup>+</sup> removal efficiency (%)	Final EC <sub>1:2</sub> (dS m <sup>-1</sup> )	Reduction in EC <sub>1:2</sub> (%)	Cumulative water flow (± 1 ml)	Energy density (kWh m <sup>-3</sup> )
E-1 (0.5 V cm <sup>-1</sup> )	36	58	45	37	3.94	24	63	35.7
E-2 (1 V cm <sup>-1</sup> )	54	71	58	54	2.07	60	94	94.4
E-3 (2 V cm <sup>-1</sup> )	71	91	64	63	1.29	75	69	218.6

where, “ $\sum_{i=1}^9 C_i$ ” is the sum of the initial concentration of ions before the EK experiments and “ $\sum_{f=1}^9 C_f$ ” is the sum of the final concentration of ions after the EK experiments.

The results reveal that at high EF, i.e., 2 V cm<sup>-1</sup>, the maximum RE of total Cr, Na<sup>+</sup>, Cl<sup>-</sup>, and K<sup>+</sup> ions was achieved at 71%, 91%, 64, and 63%, respectively, due to higher electroosmosis and electromigration as well as more energy was consumed (i.e., 218.6 kWh m<sup>-3</sup>). While, at 1 V cm<sup>-1</sup>, the RE of total Cr, Na<sup>+</sup>, Cl<sup>-</sup>, and K<sup>+</sup> ions was 54%, 71%, 58%, and 54%, respectively, and low energy was consumed 94.4 kWh m<sup>-3</sup> as compared to E-3. During E-1, the low value of EF (i.e., 0.5 V cm<sup>-1</sup>) causes low energy consumption, i.e., 35.7 kWh m<sup>-3</sup> as well as the low removal of ions. The RE of total Cr, Na<sup>+</sup>, Cl<sup>-</sup>, and K<sup>+</sup> ions was obtained 36%, 58%, 45%, and 37%, respectively. To the effective removal of ions more treatment time is required under the low EF, i.e., 0.5 V cm<sup>-1</sup>.

However, at 1 and 2 V cm<sup>-1</sup>, the more treatment time will not be beneficially because the ions removal and EOF halted due to acidic-alkaline fronts by the formation of high VG zone within the soil. We concluded that the effectiveness of the EK process also depends on the maintenance of the EOF rate for a long time; therefore, more treatment time is required to obtain the higher removal of ions. This may be achieved by inhibiting the pH fronts within the soil with the proper flushing solution in the electrodes and using low EF strength.

In all EK experiments, the removal of cations (Na<sup>+</sup> and K<sup>+</sup> ions) was higher than that of anions (chromate and Cl<sup>-</sup> ions) because the electromigration and the direction of EOF (from anode to cathode), while the anions migrate toward the anode by the electromigration. In addition, the Cl<sup>-</sup> ions react with Mg<sup>2+</sup> and Ca<sup>2+</sup> in the form of complexes such as (MgCl<sub>2</sub>), and (CaCl<sub>2</sub>) [39]. Although the higher EF enhances the removal of ions, at the same time it may cause the destruction of organic matter in the soil due to the joule heating effect.

At the end of each experiment, the energy density was calculated by Eq. (13) [49].

$$\text{Energy density (kWh m}^{-3}\text{)} = \frac{E}{V} \left( \int_0^t I dt \right) \quad (13)$$

where, “V” is the volume of the soil sample (cm<sup>3</sup>) “I” is the electric current (A), “t” is the treatment time (h), and “E” is

the electric potential (V). The values of energy density are given in Table 2.

The volume of each soil sample was 4.53 × 10<sup>-4</sup> m<sup>3</sup> while different electric potentials (4.5, 9, and 18 V) were applied over the 9 cm length of the soil samples. The values of energy density were 35.7, 96.4, and 218.8 kWh m<sup>-3</sup> after the E-1, E-2, and E-3 experiments, respectively. The results indicate that the RE of ions and energy density increase with the applied EF strength. Higher EF enhanced the EOF and electromigration of ions, by which higher ionic charge species were carried out of contaminated soil and accumulated in the vicinity of the anode and cathode reservoirs. We concluded that in order to save energy consumption, the EF of 0.5 V cm<sup>-1</sup> is a preferable limit for the removal of ions under high salinity area in practical conditions.

## 4 Conclusion

The aim of this research is to determine the effect of DC voltage gradient (i.e., 0.5, 1, and 2 V cm<sup>-1</sup>) on energy consumption and the removal of salt (Na<sup>+</sup>, Cl<sup>-</sup>, and K<sup>+</sup>) and heavy metal (Cr) ions from salt-affected clayey soil.

The results revealed that the higher electric field intensities resulted in more energy consumption and higher the EOF rate and electromigration process. The maximum removal of total Cr, Na<sup>+</sup>, Cl<sup>-</sup>, and K<sup>+</sup> ions was achieved 71%, 91%, 64%, and 63%, respectively, at 2 V cm<sup>-1</sup> by the higher EOF rate and electromigration. In addition, the high acidic-alkaline fronts were produced, which may affect the EOF rate and the removal of ions from contaminated soil. While in the case of lower EF, i.e., 0.5 V cm<sup>-1</sup>, the removal of total Cr, Na<sup>+</sup>, Cl<sup>-</sup>, and K<sup>+</sup> ions was achieved 36%, 58%, 45%, and 37%, respectively.

The values of energy density were 35.7, 96.4, and 218.8 kWh m<sup>-3</sup> under the EF of 0.5, 1, and 2 V cm<sup>-1</sup>, respectively. We concluded that the effectiveness of the EK process also depends on the maintenance of the EOF rate for a long time; therefore, more treatment time is required to obtain the higher removal of ions. This may be achieved by inhibiting the pH fronts within the soil with the proper flushing solution in the electrodes and using a low EF strength.

**Acknowledgements** This work was funded by the Researchers Supporting Project Number (RSP2023R441), King Saud University, Riyadh, Saudi Arabia.

**Author contributions** AAH wrote the manuscript and performed the experiment; KK contributed to supervision, investigation and edited final manuscript; MW, SU and MH contributed to experimental analysis and review of paper; MA, SMM, MAH, AAd.H and AR contributed to review the paper; All authors have read and agreed to publish the manuscript.

## Declarations

**Competing interests** The authors declare no competing interests.

## References

- Ashraf A, Bibi I, Niazi NK et al (2017) Chromium(VI) sorption efficiency of acid-activated banana peel over organo-montmorillonite in aqueous solutions. *Int J Phytoremed* 55:305–318
- Pamukcu S, Weeks A, Wittle JK (1997) Electrochemical extraction and stabilization of selected inorganic species in porous media. *J Hazard Mater* 55:305–318. [https://doi.org/10.1016/S0304-3894\(97\)00025-3](https://doi.org/10.1016/S0304-3894(97)00025-3)
- Nasiri A, Jamshidi-Zanjani A, Khodadadi Darban A (2020) Application of enhanced electrokinetic approach to remediate Cr-contaminated soil: effect of chelating agents and permeable reactive barrier. *Environ Pollut* 266:115197. <https://doi.org/10.1016/j.envpol.2020.115197>
- Fonseca B, Pazos M, Tavares T, Sanromán MA (2012) Removal of hexavalent chromium of contaminated soil by coupling electrokinetic remediation and permeable reactive biobarriers. *Environ Sci Pollut Res* 19:1800–1808. <https://doi.org/10.1007/s11356-011-0694-y>
- Whitacre DM (2015) Reviews of environmental contamination and toxicology. *Rev Environ Contam Toxicol* 233:45–69. <https://doi.org/10.1007/978-3-319-10479-9>
- Ertani A, Mietto A, Borin M, Nardi S (2017) Chromium in agricultural soils and crops: a review. *Water Air Soil Pollut.* <https://doi.org/10.1007/s11270-017-3356-y>
- Tchounwou PB, Yedjou CG, Patlolla AK, Sutton DJ (2012) Molecular, clinical and environmental toxicology volume 3: environmental toxicology. *Mol Clin Environ Toxicol* 101:133–164. <https://doi.org/10.1007/978-3-7643-8340-4>
- Sharma A, Kapoor D, Wang J et al (2020) Chromium bioaccumulation and its impacts on plants: an overview. *Plants* 9:100. <https://doi.org/10.3390/plants9010100>
- Voccianta M, Dov VG, Ferro S (2021) Sostenibilidad en Procesos de Remediación electrocinética: Un análisis crítico. pp 1–15
- Puri AN, Anand M (1936) Reclamation of alkali soils by electro-dialysis. *Soil Sci* 42:23–27
- Acar YB, Gale RJ, Alshawabkeh AN et al (1995) Electrokinetic remediation: basics and technology status. *J Hazard Mater* 40:117–137. [https://doi.org/10.1016/0304-3894\(94\)00066-P](https://doi.org/10.1016/0304-3894(94)00066-P)
- Yeung AT (2011) Milestone developments, myths, and future directions of electrokinetic remediation. *Sep Purif Technol* 79:124–132. <https://doi.org/10.1016/j.seppur.2011.01.022>
- Acar YB, Alshawabkeh AN (1993) Principles of electrokinetic remediation. *Environ Sci Technol* 27:2638–2647. <https://doi.org/10.1021/es00049a002>
- Zhou M, Xu J, Zhu S et al (2018) Exchange electrode-electrokinetic remediation of Cr-contaminated soil using solar energy. *Sep Purif Technol* 190:297–306. <https://doi.org/10.1016/j.seppur.2017.09.006>
- Wen D, Guo X, Fu R (2021) Inhibition characteristics of the electrokinetic removal of inorganic contaminants from soil due to evolution of the acidic and alkaline fronts. *Process Saf Environ Prot* 155:343–354. <https://doi.org/10.1016/j.psep.2021.09.030>
- Yeung AT, Gu YY (2011) A review on techniques to enhance electrochemical remediation of contaminated soils. *J Hazard Mater* 195:11–29. <https://doi.org/10.1016/j.jhazmat.2011.08.047>
- Mena E, Villaseñor J, Cañizares P, Rodrigo MA (2016) Effect of electric field on the performance of soil electro-bioremediation with a periodic polarity reversal strategy. *Chemosphere* 146:300–307. <https://doi.org/10.1016/j.chemosphere.2015.12.053>
- Pamukcu S, Kenneth Wittle J (1992) Electrokinetic removal of selected heavy metals from soil. *Environ Progress Electrokinet Remov Sel Heavy Met oil* 11:241–250. <https://doi.org/10.1002/ep.670110323>
- Wen D, Fu R, Li Q (2021) Removal of inorganic contaminants in soil by electrokinetic remediation technologies: a review. *J Hazard Mater* 401:123345. <https://doi.org/10.1016/j.jhazmat.2020.123345>
- Reddy KR, Cameselle C (2009) Technologies for polluted soils, sediments and groundwater. Wiley, Hoboken
- Juwarkar AA, Singh SK, Mudhoo A (2010) A comprehensive overview of elements in bioremediation. *Rev Environ Sci Biotechnol* 9:215–288. <https://doi.org/10.1007/s11157-010-9215-6>
- Abou-Shady A (2016) Reclaiming salt-affected soils using electro-remediation technology: PCPSS evaluation. *Electrochim Acta* 190:511–520. <https://doi.org/10.1016/j.electacta.2016.01.036>
- Luo Q, Wang H, Zhang X et al (2006) In situ bioelectrokinetic remediation of phenol-contaminated soil by use of an electrode matrix and a rotational operation mode. *Chemosphere* 64:415–422. <https://doi.org/10.1016/j.chemosphere.2005.11.064>
- Xu W, Wang C, Liu H et al (2010) A laboratory feasibility study on a new electrokinetic nutrient injection pattern and bioremediation of phenanthrene in a clayey soil. *J Hazard Mater* 184:798–804. <https://doi.org/10.1016/j.jhazmat.2010.08.111>
- Bessaim MM, Missoum H, Bendani K et al (2020) Sodic-saline soil remediation by electrochemical treatment under uncontrolled pH conditions. *Arab J Geosci* 13:199. <https://doi.org/10.1007/s12517-020-5210-6>
- Mena E, Villaseñor J, Rodrigo MA, Cañizares P (2016) Electrokinetic remediation of soil polluted with insoluble organics using biological permeable reactive barriers: effect of periodic polarity reversal and voltage gradient. *Chem Eng J* 299:30–36. <https://doi.org/10.1016/j.ccej.2016.04.049>
- Hu W, Cheng WC, Wen S (2023) Investigating the effect of degree of compaction, initial water content, and electric field intensity on electrokinetic remediation of an artificially Cu- and Pb-contaminated loess. *Acta Geotech* 18:937–949. <https://doi.org/10.1007/s11440-022-01602-9>
- Zhu S, Zhu D, Wang X (2017) Removal of fluorine from red mud (bauxite residue) by electrokinetics. *Electrochim Acta* 242:300–306. <https://doi.org/10.1016/j.electacta.2017.05.040>
- Yu X, Muhammad F, Yan Y et al (2019) Effect of chemical additives on electrokinetic remediation of Cr-contaminated soil coupled with a permeable reactive barrier. *R Soc Open Sci* 6:182138. <https://doi.org/10.1098/rsos.182138>
- Hussain AA, Kamran K, Ishaq M et al (2023) Optimization of electroosmotic flow to enhance the removal of contaminants from low-permeable soils. *J Appl Electrochem* 53:1245–1258. <https://doi.org/10.1007/s10800-023-01845-8>
- Estefan G, Sommer R, Ryan J (2013) Methods of soil, plant, and water analysis: a manual for the West Asia and North Africa Region. *Int Cent Agric Res Dry Areas* 40:83–89
- Ishaq M, Kamran K, Jamil Y, Sarfraz RA (2021) Electric potential and current distribution in contaminated porous building materials

- under electrokinetic desalination. *Mater Struct* 54:175. <https://doi.org/10.1617/s11527-021-01770-2>
33. Weng CH, Lin YT, Lin TY, Kao CM (2007) Enhancement of electrokinetic remediation of hyper-Cr(VI) contaminated clay by zero-valent iron. *J Hazard Mater* 149:292–302. <https://doi.org/10.1016/j.jhazmat.2007.03.076>
  34. Sun TR, Ottosen LM, Jensen PE (2012) Pulse current enhanced electro-dialytic soil remediation-comparison of different pulse frequencies. *J Hazard Mater* 237–238:299–306. <https://doi.org/10.1016/j.jhazmat.2012.08.043>
  35. Beretta AN, Silbermann AV, Paladino L et al (2014) Análisis de textura del suelo con hidrómetro: modificaciones al método de Bouyoucos. *Sci Investig Agrar* 41:263–271. <https://doi.org/10.4067/S0718-16202014000200013>
  36. Zhu S, Han D, Zhou M, Liu Y (2016) Ammonia enhanced electrokinetics coupled with bamboo charcoal adsorption for remediation of fluorine-contaminated kaolin clay. *Electrochim Acta* 198:241–248. <https://doi.org/10.1016/j.electacta.2016.03.033>
  37. Kamran K, Van Soestbergen M, Huinink HP, Pel L (2012) Inhibition of electrokinetic ion transport in porous materials due to potential drops induced by electrolysis. *Electrochim Acta* 78:229–235. <https://doi.org/10.1016/j.electacta.2012.05.123>
  38. Wang T, Liu Y, Wang J et al (2019) In-situ remediation of hexavalent chromium contaminated groundwater and saturated soil using stabilized iron sulfide nanoparticles. *J Environ Manag* 231:679–686. <https://doi.org/10.1016/j.jenvman.2018.10.085>
  39. Bessaim MM, Missoum H, Bendani K et al (2020) Effect of processing time on removal of harmful emerging salt pollutants from saline-sodic soil during electrochemical remediation. *Chemosphere* 253:126688. <https://doi.org/10.1016/j.chemosphere.2020.126688>
  40. Ait Ahmed O, Derriche Z, Kameche M et al (2016) Electro-remediation of lead contaminated kaolinite: an electro-kinetic treatment. *Chem Eng Process Process Intensif* 100:37–48. <https://doi.org/10.1016/j.ccep.2015.12.002>
  41. Hussain AA, Kamran K, Hina M et al (2023) Effect of electrokinetic treatment time on energy consumption and salt ions removal from clayey soils. *Mater Res Express* 10:055505. <https://doi.org/10.1088/2053-1591/acd436>
  42. Pamukcu S, Weeks A, Wittle JK (2004) Enhanced reduction of Cr(VI) by direct electric current in a comminated clay. *Environ Sci Technol* 38:1236–1241. <https://doi.org/10.1021/es034578v>
  43. Meng F, Wang Y, Leng L, Wang J (2012) Effect of applied voltage on the electrokinetic removal of chromium from soils. *Adv Mater Res* 414:144–149. <https://doi.org/10.4028/www.scientific.net/AMR.414.144>
  44. Soliemanzadeh A, Fekri M (2017) The application of green tea extract to prepare bentonite-supported nanoscale zero-valent iron and its performance on removal of Cr(VI): effect of relative parameters and soil experiments. *Microporous Mesoporous Mater* 239:60–69. <https://doi.org/10.1016/j.micromeso.2016.09.050>
  45. Ukhurebor KE, Aigbe UO, Onyancha RB et al (2021) Effect of hexavalent chromium on the environment and removal techniques: a review. *J Environ Manag* 280:111809. <https://doi.org/10.1016/j.jenvman.2020.111809>
  46. Yan Y, Li H, Yu X et al (2019) Efficient removal of chromium from soil in a modified electrokinetic system using iron-treated activated carbon as third electrode. *J Taiwan Inst Chem Eng* 101:15–23. <https://doi.org/10.1016/j.jtice.2019.03.021>
  47. Kim KJ, Cho JM, Baek K et al (2010) Electrokinetic removal of chloride and sodium from tidelands. *J Appl Electrochem* 40:1139–1144. <https://doi.org/10.1007/s10800-010-0082-1>
  48. Feijoo J, Nóvoa XR, Rivas T, Ottosen LM (2018) Enhancing the efficiency of electrochemical desalination of stones: a proton pump approach. *Mater Struct Constr*. <https://doi.org/10.1617/s11527-018-1224-x>
  49. Li X, Wang L, Sun X, Cong Y (2019) Analysis of mobilization of inorganic ions in soil by electrokinetic remediation. *Front Struct Civ Eng* 13:1463–1473. <https://doi.org/10.1007/s11709-019-0569-8>

**Publisher's Note** Springer Nature remains neutral with regard to jurisdictional claims in published maps and institutional affiliations.

Springer Nature or its licensor (e.g. a society or other partner) holds exclusive rights to this article under a publishing agreement with the author(s) or other rightsholder(s); author self-archiving of the accepted manuscript version of this article is solely governed by the terms of such publishing agreement and applicable law.

## Authors and Affiliations

Abdul Ahad Hussain<sup>1,2</sup> · Kashif Kamran<sup>1</sup> · Muhammad Waseem<sup>1</sup> · Shahwar Umar<sup>1</sup> · Maryam Hina<sup>3</sup> · Muhammad Altaf<sup>4</sup> · Sura Mohammad Mohealdeen<sup>5</sup> · Mohamed A. Habila<sup>6</sup> · Ali Adhab Hussein<sup>7</sup> · Aisha Rafique<sup>1</sup>

✉ Abdul Ahad Hussain  
ahadahad.uaf@gmail.com

✉ Kashif Kamran  
k.kamran@uaf.edu.pk

<sup>1</sup> Department of Physics, University of Agriculture Faisalabad, Faisalabad 38040, Pakistan

<sup>2</sup> School of Energy and Power Engineering, Dalian University of Technology, Dalian 116024, China

<sup>3</sup> Institute of Physics, Bahauddin Zakariya University, Multan 60800, Pakistan

<sup>4</sup> Department of Chemistry, Center of Excellence for Innovation in Chemistry (PERCH-CIC), Chiang Mai University, Chiang Mai 50200, Thailand

<sup>5</sup> Department of Radiology & Sonar Techniques, Al-Noor University College, Nineveh, Iraq

<sup>6</sup> Department of Chemistry, College of Science, King Saud University, P. O. Box 2455, Riyadh 11451, Saudi Arabia

<sup>7</sup> Department of Medical Laboratory Technics, Al-Zahrawi University College, Karbala, Iraq